

Interactions of π^+ Mesons with Protons at 2.08 BeV/c*

FREDERICK E. JAMES† AND HENRY L. KRAYBILL

Yale University, New Haven Connecticut and Brookhaven National Laboratory, Upton, New York

(Received 20 September 1965)

Interactions of 2.08-BeV/c positive pions with protons have been studied using the 20-in. hydrogen bubble chamber and the alternating gradient synchrotron at Brookhaven National Laboratory. Using 3000 elastic and 8000 inelastic events, the partial cross sections for elastic scattering and for meson production have been measured. The ρ^+ , ρ^0 , ω^0 , and η^0 resonances are produced strongly and emerge predominantly in the forward direction in the center-of-mass system, suggesting a peripheral mechanism for their production. The possibility of explaining these reactions by specific particle-exchange models is investigated. More than 75% of the ρ^0 , ω^0 , and η^0 are produced with the N_{33}^* (1238) isobar. The N^* (1688) is produced in about one-third of the $\pi^+\pi^+N$ final states. Cross sections for production of ρ^+p , $\pi^+p\omega$, $N_{33}^*\omega$, $\pi^+p\eta$, $N_{33}^*\eta$, $\pi^+p\rho^0$, $N_{33}^*\rho^0$, $N_{16}^*\pi^+$, and $N_{33}^*\pi^0$, are given. A_1 , B , ϕ , and X mesons are not observed.

I. INTRODUCTION

WE report here the results of a study of pion production in π^+ -proton collisions at momentum 2.08 BeV/c. Using pictures taken in the Brookhaven 20-in. hydrogen chamber at the alternating gradient synchrotron at Brookhaven National Laboratory, we have analyzed 3200 elastic and 5500 inelastic two-pronged interactions and 2600 four-pronged interactions. Only six six-pronged interactions which did not contain obvious Dalitz pairs were found, and these were not analyzed.

The N^* (1238), N^* (1668), η , ρ , ω , ϕ , B , X , and A resonant states have been previously observed in π^+ interactions at various energies.¹⁻¹⁷ In this work we

have determined cross sections for production of the η , ρ , and ω mesons, and for associated production of the $\eta^0N_{33}^*$, $\omega^0N_{33}^*$, and $\rho^0N_{33}^*$ intermediate states, as well as for multiple pion final states. From available data, we have constructed excitation curves for production of these states from the π^+p interaction. At 2.08 BeV/c, we have found more than 75% production of N_{33}^* in each of the states $\eta\pi^+p$, $\rho^0\pi^+p$, and $\omega\pi^+p$. We have determined production and decay angular distributions for ηN_{33}^* , $\rho^0 N_{33}^*$, and ωN_{33}^* , and have considered the ability of currently proposed production models to explain these distributions. We have searched unsuccessfully for other reported resonances accessible at this momentum, namely the B , ϕ , X , and A_1 mesons. Other phenomena, such as a strong final-state interaction in the $\pi^+\pi^+N$ state, were discussed briefly. The angular distribution of the elastic scattering has been published elsewhere.¹⁸

II. EXPERIMENTAL PROCEDURE

The analysis was conducted on 40 000 pictures of π^+ mesons from separated beam No. 1¹⁹ at the alternating gradient synchrotron. The mean momentum was determined to be 2.077 BeV/c, by making four-constraint kinematic fits to interactions identified as $\pi^+ + p \rightarrow \Sigma^+ + K^+$. The momentum distribution of the beam had a spread of $\pm 1.6\%$.

Phys. Rev. 138, B897 (1965); Phys. Letters 10, 226, 229 (1964); 11, 167 (1964).

¹⁴ G. Goldhaber, J. Brown, S. Goldhaber, J. Kadyk, B. Shen, and G. Trilling, Phys. Rev. Letters 12, 336 (1964); G. Goldhaber, S. Goldhaber, J. Kadyk, B. Shen, and G. Trilling, *ibid.* 12, 336 (1964); G. Goldhaber, S. Goldhaber, J. Kadyk, and B. Shen, *ibid.* 15, 118 (1965).

¹⁵ H. Cohn, W. Bugg, and G. Condo, Phys. Rev. Letters 15, 344 (1965).

¹⁶ F. Bruyant, M. Goldberg, M. Holder, M. Kramer, J. Major, G. Vegni, H. Wingeler, P. Fleury, J. Huc, R. Lestienne, G. DeRosny, and R. Vanderhaghen, Phys. Letters 10, 232 (1964).

¹⁷ M. Deutschmann, R. Schulte, H. Weber, W. Woischnig, C. Grote, J. Klugow, S. Nowak, S. Brandt, V. Cocconi, O. Czyzewski, P. Dalpiaz, G. Kellner, and D. Morrison, Phys. Letters 12, 356 (1964).

¹⁸ F. James, J. Johnson, and H. Kraybill, Phys. Letters 19, 72 (1965).

¹⁹ C. Baltay, J. Sandweiss, J. Sanford, H. Brown, M. Webster, and S. Yamamoto, Nucl. Instr. Methods 20, 37 (1963).

* Supported in part by the U. S. Atomic Energy Commission and by the National Science Foundation.

† Present address: Institut du Radium, Paris, France.

¹ D. Stonehill and H. Kraybill, Rev. Mod. Phys. 34, 503 (1962).

² H. Foelsche and H. Kraybill, Phys. Rev. 134, B1138 (1964).

³ R. Kraemer, L. Madansky, M. Meer, M. Nussbaum, A. Pevsner, C. Richardson, R. Strand, R. Zdanis, T. Fields, S. Orenstein, and T. Toohig, Phys. Rev. 136, B496 (1964).

⁴ F. Crawford, R. Grossman, L. Lloyd, L. Price, and E. Fowler, Phys. Rev. Letters 11, 564 (1963); 10, 110 (1963). F. Crawford, L. Lloyd, and E. Fowler, *ibid.* 10, 546 (1963).

⁵ M. Foster, M. Peters, R. Hartung, R. Matsen, D. Reeder, M. Good, M. Meer, F. Loeffler, and R. McIlwain, Phys. Rev. 138, B652 (1965).

⁶ D. Carmony and R. Van de Walle, Phys. Rev. Letters 8, 73 (1962). J. Anderson, V. Bang, P. Burke, D. Carmony, and N. Schmitz, Rev. Mod. Phys. 33, 431 (1961).

⁷ R. Barloutaud, J. Heughebaert, A. Leveque, C. Louedec, J. Meyer, and D. Tycho, Nuovo Cimento 27, 238 (1963).

⁸ L. Fortney, J. Chapman, E. Fowler, P. Connolly, E. Hart, P. Hough, and R. Strand, Bull. Am. Phys. Soc. 9, 420 (1964).

⁹ L. Auerbach, T. Elioff, W. Johnson, J. Lach, C. Wiegand, and T. Ypsilantis, Phys. Rev. Letters 9, 173 (1962).

¹⁰ C. Alff, D. Berley, D. Colley, N. Gelfand, U. Nauenberg, D. Miller, J. Schultz, J. Steinberger, T. Tan, H. Brugger, and R. Plano, Phys. Rev. Letters 9, 322, 325 (1962).

¹¹ Saclay-Orsay-Bari-Bologna collaboration, Nuovo Cimento 37, 361 (1965); Phys. Letters 11, 347, (1964).

¹² M. Abolins, D. Carmony, D. Hoa, R. Lander, C. Rindfleisch, and N. Xuong, Phys. Rev. 136, B195 (1964). N. Xuong, R. Lander, W. Mehlhop, and P. Yager, Phys. Rev. Letters, 11, 227 (1963); M. Abolins, R. Lander, W. Mehlhop, and N. Xuong, *ibid.* 11, 381 (1963); R. Lander, M. Abolins, D. Carmony, T. Hendricks, N. Xuong, and P. Yager, *ibid.* 13, 346 (1964).

¹³ Aachen-Berlin-Birmingham-Bonn-Hamburg-London-Munich collaboration, Nuovo Cimento 34, 495 (1964); 35, 659 (1965);

Because of the measured efficiency of the beam separators, contamination of the beam by protons is believed negligible. A computation of μ^+ contamination yields $(7.1_{-2.3}^{+0.2})\%$. Therefore, in computing cross sections, 6% muon contamination was assumed.

The chamber was operated so that a minimum ionizing track would produce about 12 bubbles/cm. Under these conditions, visual estimates of ionization in the range of 1 to 3 times minimum have an error less than 50% with about 90% confidence.

Two complete and separate scans were made of all pictures, to find two-pronged, four-pronged, and six-pronged interactions. All events found were measured and identification was attempted. The first scan found 94% of the two-pronged events and 93% of the four-pronged events found by both scans. The second scan found about 90% of the events found by both scans. It was assumed that both scans together found essentially 100% of the events, except for the events in the forward peak of the elastic scattering, for which a separate correction was made.

The number of beam tracks was counted in every tenth picture by the scanners. This count was checked by a careful control count of selected rolls, from which it differed by less than 2%.

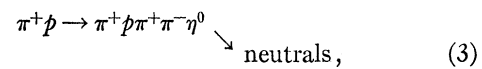
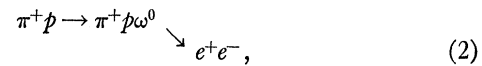
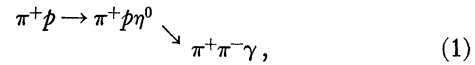
All two-pronged and four-pronged interactions within a fiducial volume approximately 25 cm in length along the beam were measured with the Yale precision measuring machines. Usually five points were measured on each track in each view of the pair which was most favorable for stereographic reconstruction.

The completed measurements were passed through a diagnostic program which reconstructed each track and indicated which events were to be remeasured because of incorrect data. Rejection usually occurred because the overconstrained fit of a track to a helix was not sufficiently close.

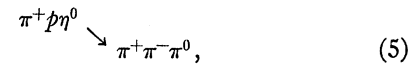
Acceptable measurements were passed through the Yale reconstruction and kinematic analysis program (YACK), written by Professor Horace D. Taft. Both kinematic fitting and estimates of bubble density were used for all events in order to determine particle and reaction identifications. An event which fitted a four-constraint interpretation with $\chi^2 < 40$ was identified as such, provided the bubble density of all tracks was consistent with the interpretation. An event which was not consistent with a four-constraint interpretation but which made a one-constraint fit with $\chi^2 < 8$ was accepted as such provided the bubble density was judged also to be consistent with the interpretation. A few events made more than one fit; still fewer of these were also ambiguous by ionization. For such events the fit with lowest χ^2 value was chosen. The resulting one-constraint χ^2 values require a stretching factor of 1.10. The four-constraint χ^2 values require a stretching factor of 1.92. The larger correction factor for four-constraint fits has been observed in other experiments and apparently is

caused by systematic errors and distortions in the reconstruction of events.

Sixty-nine four-pronged events were not consistent with any fit. Twenty-one of these were consistent with having more than one missing neutral particle; the others presumably contain very large errors, scatters, or measuring blunders. A search was made of these events for the following reactions:



Five events were consistent with reaction (1) but this is about the number expected if there actually were no examples of that reaction. Since reaction (1) is known to occur,^{4,5} we conclude that it has been misidentified as



in most cases.

No examples were found of the other three interpretations. One such event would correspond to a cross section of about $2 \mu\text{b}$.

III. CROSS-SECTION DETERMINATIONS

The cross sections are computed as

$$\sigma = MN/2N_0\rho L,$$

where N is the number of interactions, M is the molecular weight of H_2 , N_0 is Avogadro's number, ρ is the density of liquid hydrogen, taken as 0.062 g/cm^3 , and L is the beam track length.

Our average beam track length in the fiducial region is $24.2 \pm 0.1 \text{ cm}$, and the total track length is $1.28 \times 10^5 \text{ m}$.

In determining the number of events and the beam track lengths several corrections are required.

(1) The computed beam contamination of 6% muons requires a correction of 6% in all cross sections.

(2) A correction of 6% was applied to the two-prongs, and 7% to the four-prongs, for scanning efficiency.

(3) Correction is required for missed small angle elastic scatters. The π^+ scattering peaks strongly forward. Because the pion has spin zero and the protons are not polarized, the cross section is independent of the azimuthal scattering angle (ψ). Figure 1 is a scattergram of $\cos\theta$ versus ψ for all observed elastic events. The distribution lacks events with $\cos\theta$ between -0.98 and -1.0 ; it is isotropic in ψ , except for a lack

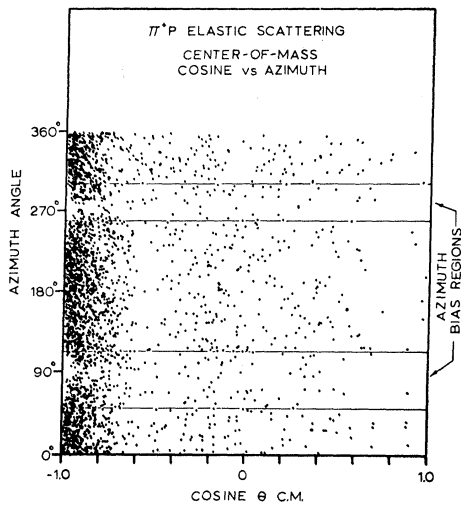


FIG. 1. Scattergram of $\cos\theta$ versus ψ for π^+p elastic scattering at 2.08 BeV/c. θ is the angle between the scattered π^+ and the beam direction in the center of mass. ψ is the azimuth of the scattering plane. $\psi=0$ corresponds to a plane parallel to the face of the chamber.

of events in two bands near $\psi=90^\circ$ and $\psi=270^\circ$. Both the bias in $\cos\theta$ and the bias in ψ represent events in which the scattering angle of the π^+ , projected onto the plane of the film, is very small, and the proton recoil

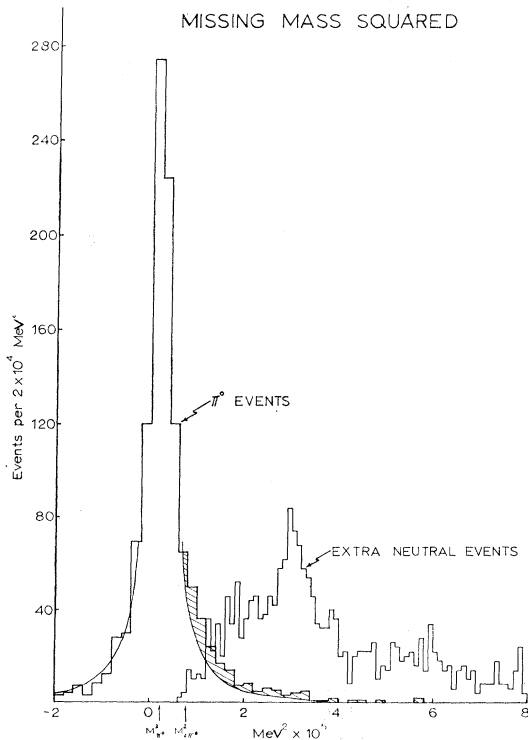


FIG. 2. Missing mass squared for events whose charged tracks were identified as π^+p , showing bias in favor of identifying events as having a single missing π^0 . Events identified as elastic scattering are not shown here.

is very short. We have determined the number of missed events by extrapolating from nonbiased regions into biased regions, assuming isotropy in ψ and exponential dependence on $\cos\theta$ near $\cos\theta=1.0$. The correction for forward scatters is $(22.2 \pm 2.0)\%$ of observed elastic events. This number does not depend strongly on the exact shape assumed for the forward diffraction peak.

(4) Identification biases: We consider the missing mass squared spectrum for events identified as $\pi^+p\pi^0$. This should be a peak symmetric about m_{π^2} , plus background due to misidentified elastic collisions and events with more than one π^0 . The experimental distribution in Fig. 2 has a larger tail toward high masses than toward low masses. If we make the spec-

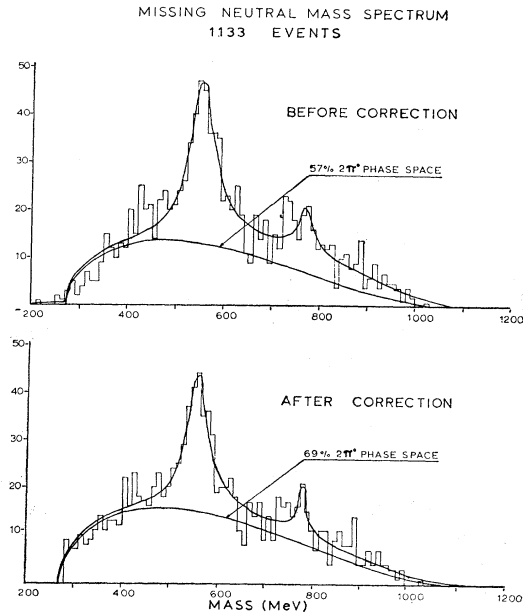


FIG. 3. Missing neutral mass spectrum for events whose charged tracks were identified as π^+p , excluding elastic scattering events and $\pi^+p\pi^0$ events, before and after correction for bias mentioned in Fig. 2.

trum symmetric by removing events from the high-mass portion and adding them to the corresponding spectrum for events identified as having more than one missing π^0 , we find that the latter spectrum more nearly acquires the expected shape of the $2\pi^0$ phase space (see Fig. 3). From this result and from the fact that the square of the missing mass for elastic events is distributed as expected, we judge that no other correction is needed for $\pi^+p\pi^0$ misidentification. This correction is 6.7% of the events identified as $\pi^+p\pi^0$.

For $\pi^+\pi^+n$ events (see Fig. 4) the neutron mass is better resolved than the π^0 mass, and no correction for misidentification was needed.

Because the residual energy in four-pronged reactions is low, there are very few ambiguous events, and no

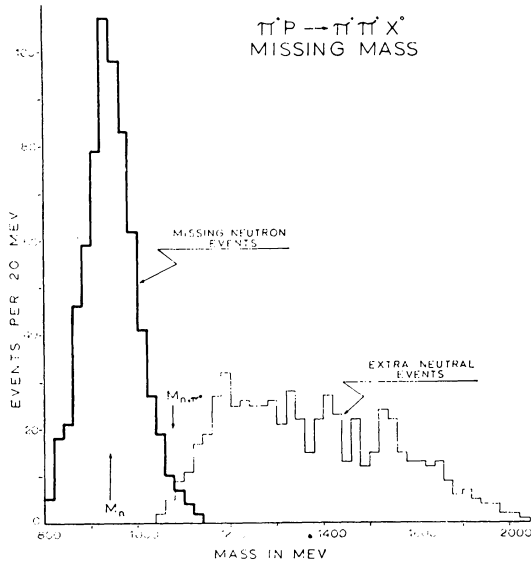


FIG. 4. Missing mass for events whose charged tracks were identified as $\pi^+\pi^+$, separated into events fitting the hypothesis $\pi^+\pi^+n$, and events not fitting this interpretation (chi-squared cutoff=8).

correction for misidentification is required. The missing mass squared for identified $\pi^+p\pi^+\pi^-\pi^0$ events is shown in Fig. 5.

The cross sections are given in Table I. The strange-particle cross sections were determined from the same

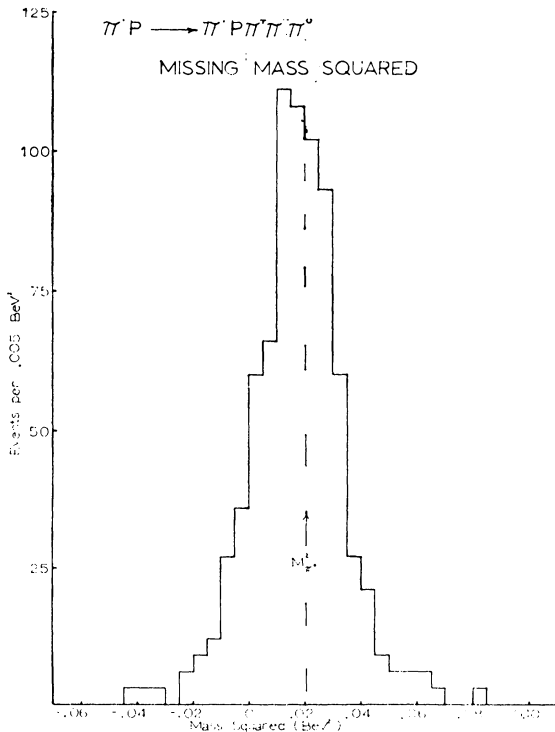


FIG. 5. Missing mass squared for events identified as $\pi^+p \rightarrow \pi^+p\pi^+\pi^-\pi^0$.

TABLE I. π^+p cross sections at 2.08 BeV/c.

Final state	Number of events		Cross section	
	Actual	Corrected	(Millibarns)	Error
π^+p	3197	4471	9.46	0.40
$\pi^+p\pi^0$	2298	2499	5.29	0.13
π^+p neutrals	1197	1565	3.32	0.11
$\pi^+\pi^+n$	930	1064	2.25	0.09
$\pi^+\pi^+n\pi^0$	674	771	1.63	0.07
$\pi^+p\pi^+\pi^-$	1140	1641	3.40	0.11
$\pi^+p\pi^+\pi^-\pi^0$	1021	1163	2.41	0.09
$\pi^+\pi^+\pi^+\pi^-n$	110	125	0.26	0.03
$\pi^+p\pi^+\pi^-\pi^+\pi^-$	6	8	0.01	
Strange particles	304	360	0.72	0.07
Total			28.75	± 1.00

film by Foelsche *et al.*²⁰ The errors in Table I are statistical, except for the error in the total cross section, which is the sum of 1% statistical error, 1% uncertainty in the density of the liquid hydrogen, and 1% uncertainty in the beam count. The total cross section agrees well with the more accurate counter data of Diddens *et al.*²¹ who report 29.2 ± 0.3 mb.

IV. SINGLE-PION PRODUCTION

A. The Reaction $\pi^+p \rightarrow \pi^+p\pi^0$

Figure 6 shows a Dalitz plot for the final state $\pi^+p\pi^0$. The ρ^+ resonance appears as a band running from lower right to upper left, crossing the two isobar bands. There is an extensive region where events lie in both ρ^+ and N_{33}^{*++} peaks. This difficulty has seriously hampered attempts to analyze ρ^+ production at lower

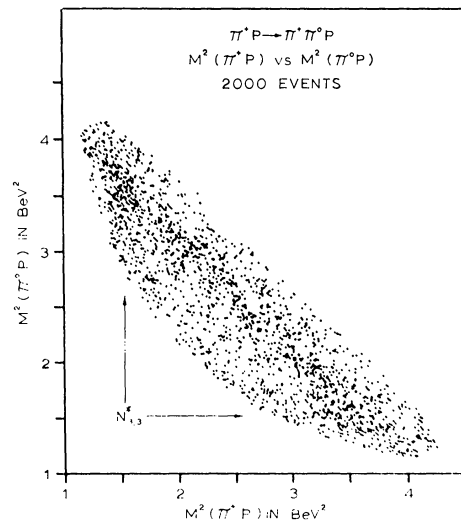


FIG. 6. Dalitz plot for single π^0 production: $M^2(p,\pi^+)$ versus $M^2(p,\pi^0)$.

²⁰ H. Foelsche, A. Lopez-Cepero, C. Y. Chien, and H. Kraybill, in *Proceedings of the International Conference on High Energy Physics, Dubna, 1964* (Atomizdat, Moscow, 1965).

²¹ A. Diddens, E. Jenkins, T. Kycia, and K. Riley, *Phys. Rev. Letters* **10**, 262 (1963).

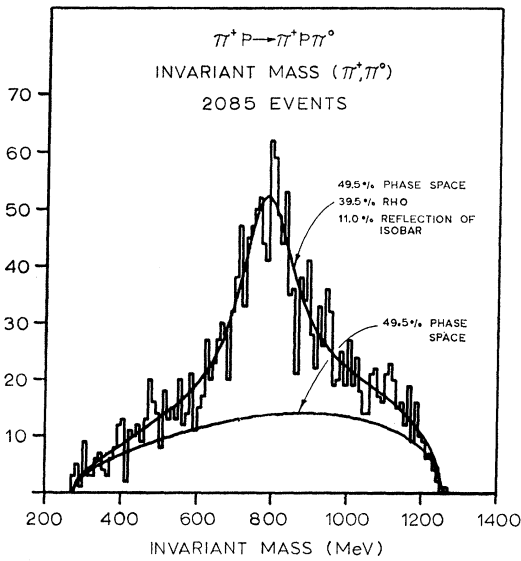


FIG. 7. Invariant mass spectrum of $\pi^+\pi^0$ in single π^0 production events. The fitted rho mass is 783 MeV and full width is 177 MeV.

energies,¹ where isobar production is stronger and the allowed region of the Dalitz plot is smaller.

To determine the masses, widths, and amount of the resonances, we have neglected possible interference between resonances and have fitted each mass spectrum with a sum of unweighted phase space, phase space weighted by a Breit-Wigner resonance, and a "reflection" caused by the other resonance. We used the resonance shape:

$$W = k / [(M - M_0)^2 + (\Gamma/2)^2].$$

Parameters varied in fitting were the mass (M_0), full width (Γ), and amount of each resonance. The following values gave the best fit:

$\pi^+\pi^0$ invariant mass: (see Fig. 7)

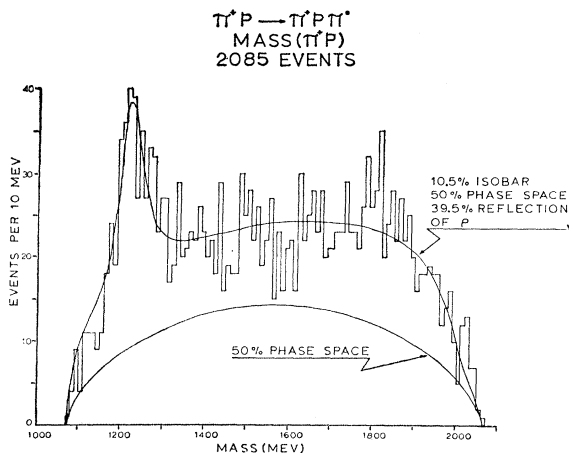


FIG. 8. Invariant mass spectrum of π^+p in single π^0 production events. The fitted isobar mass is 1219 MeV and full width is 66 MeV.

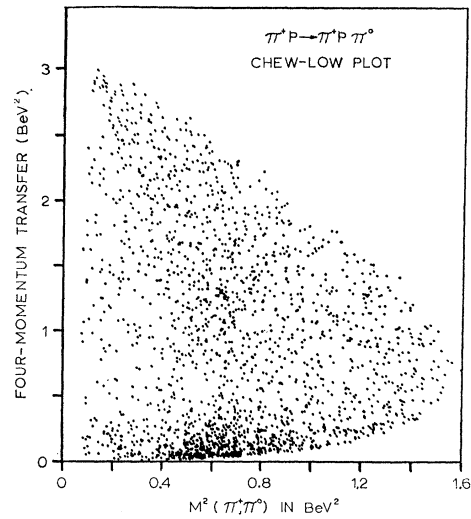


FIG. 9. Chew-Low plot for single π^0 production events: $M^2(\pi^+\pi^0)$ versus Δ^2 (to p).

amount of ρ^+	(39.5 ± 2.0)%
phase space	(49.5 ± 2.0)%
reflection of isobar fixed at 11.0%	
ρ^+ mass	783 ± 6 MeV
ρ^+ width	117 ± 15 MeV

π^+p invariant mass: (see Fig. 8)

percentage of isobar	(10.5 ± 1.2)%
phase space	(50.0 ± 1.2)%
reflection of ρ^+ fixed at	39.5%
isobar mass	1219 ± MeV
isobar width	66 ± 11 MeV

From the above percentages and Table I we compute the cross sections:

$\pi^+p \rightarrow \rho^+p$	2.07 ± 0.15 mb
$\pi^+p \rightarrow N_{33}^*\pi^0$	0.55 ± 0.08 mb.

The masses and widths derived from fitting the mass spectra do not agree well with the accepted values;

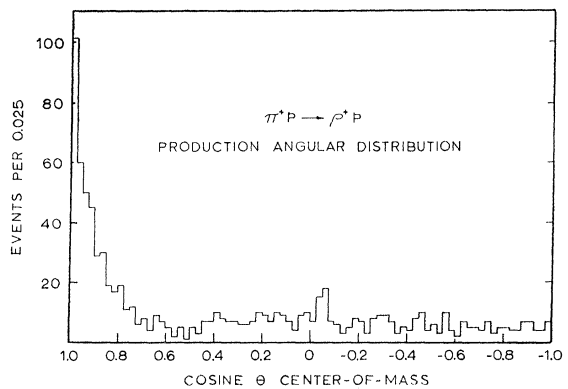


FIG. 10. Center-of-mass angular distribution of rho in reaction $\pi^+p_s \rightarrow \rho^+p$. Cosine = +1 corresponds to forward ρ .

our model is too simple. Several effects can cause the mass spectrum near a resonance to deviate from the simple Breit-Wigner shape.^{22,23} Of these effects, we judge final-state interactions to be important for the ρ^+ . Figure 9 shows a scattergram in which the square of the invariant mass of $(\pi^+\pi^0)$ is plotted against the square of the four-momentum transfer (Δ^2) to the proton.²⁴ There is a strong clumping of events at the ρ^+ mass for the lowest allowed values of Δ^2 . This indicates²⁴ that the ρ^+ is made primarily in peripheral collisions. This is also shown by the generally forward direction of the ρ^+ in the center of mass (Fig. 10).

Since the ρ^+ has such a short lifetime ($\approx 5 \times 10^{-24}$ sec) it often decays while still close enough to the proton for its decay products to interact strongly with it, causing its measured properties to differ from its intrinsic properties. This difficulty can be alleviated by producing the ρ^+ far from the proton. We can obtain large impact parameters by choosing events in which momentum transfer to the proton is low. Therefore, for several different upper limits of Δ^2 we have fitted the $\pi^+\pi^0$ mass spectrum, using appropriately modified phase space. The results (Fig. 11) show a sudden tendency toward the usually accepted values of mass

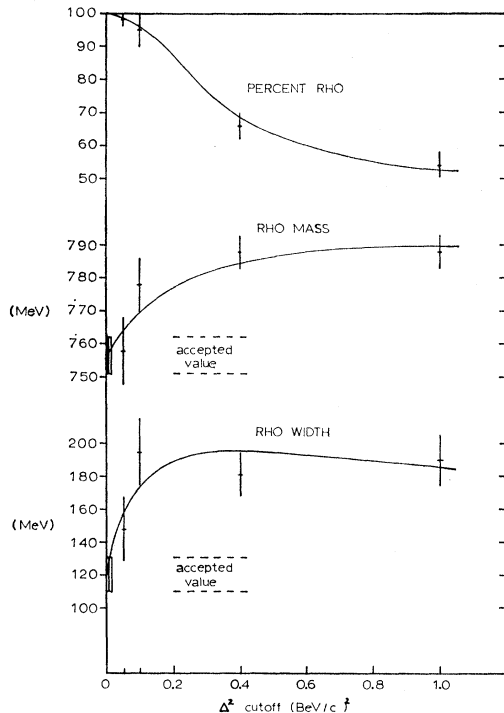


FIG. 11. Variation of mass and width of rho as a function of cutoff in four-momentum transfer to proton in reaction $\pi^+p \rightarrow \pi^+p\pi^0$. The smooth curves have been drawn arbitrarily to pass through the measured points.

²² J. D. Jackson, CERN report (unpublished); J. D. Jackson, Rev. Mod. Phys. **37**, 484 (1965).

²³ M. H. Ross and G. L. Shaw, Phys. Rev. Letters **12**, 627 (1964).

²⁴ G. Chew and F. Low, Phys. Rev. **113**, 1640 (1959).

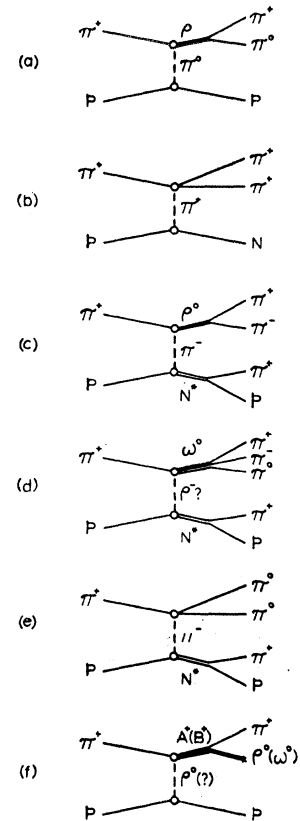


FIG. 12. Single-particle exchange diagrams.

and width when the Δ^2 cutoff is reduced below a few pion masses squared. This effect has been predicted by Ross and Shaw.²³

It is generally assumed that the reaction $\pi^+p \rightarrow \rho^+p$ occurs chiefly via single-pion exchange [see Fig. 12(a)]. Several attempts^{23,25-29} have been made to predict the production and decay angular distributions, by computing the matrix elements at the two vertices. By introducing a "form factor" at each vertex, Ferrari and Selleri have achieved remarkable agreement with experiments.^{25,26} However, objections have been raised^{28,29} that the Ferrari-Selleri amplitudes for certain partial-wave states can exceed the unitarity limit, and that the "form factors" necessary to obtain the observed angular distribution have unreasonable momentum transfer dependence. More recent calculations of the single pion exchange contribution have been made²⁸⁻³⁰ using the complete S matrix, taking account of absorption of low partial waves into other channels. In particular, Chiu and Durand have calculated²⁸ the

²⁵ E. Ferrari and F. Selleri, Nuovo Cimento **27**, 1450 (1963); **28**, 454 (1963).

²⁶ E. Ferrari, Nuovo Cimento **30**, 240 (1963).

²⁷ F. Salzman and G. Salzman, Phys. Rev. **120**, 599 (1961).

²⁸ L. Durand and Y. Chiu, Phys. Rev. Letters **12**, 399 (1964); Phys. Rev. **137**, B1530 (1965); **139**, B646 (1965).

²⁹ J. Jackson, Nuovo Cimento **25**, 1037 (1962); K. Gottfried and J. D. Jackson, *ibid.* **33**, 309 (1964); **34**, 734 (1964).

³⁰ A. Dai and W. Tobocman, Phys. Rev. Letters **12**, 511 (1964).

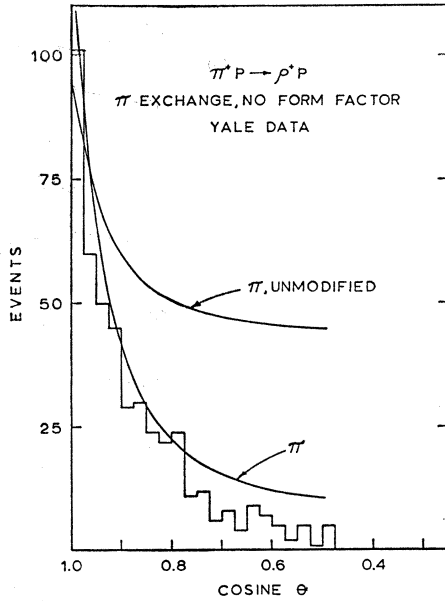


FIG. 13. The forward ρ peak in Fig. 11 with the corresponding calculation of single π^0 exchange contribution by Durand and Chiu. The upper curve is before correction for "exceptional terms" and the lower curve is after the correction.

expected ρ^+ angular distribution for our energy. They find that if they correct for certain "exceptional" or unitarity-violating terms in their expansion, they obtain a greatly improved fit to the data. This is shown by the curve marked " π " in Fig. 13.

Further evidence for the one-pion exchange character of this reaction comes from the test proposed by Treiman and Yang,³¹ who have pointed out that if a reaction proceeds through the exchange of a spinless particle, the angle between the scattering planes at the two vertices must be distributed isotropically. The Treiman-Yang distribution for our ρ^+ events [Fig. 25(b)] is consistent with isotropy.

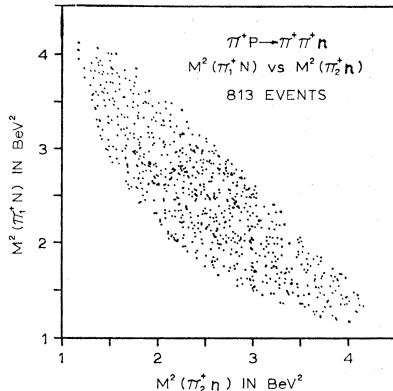


FIG. 14. Dalitz plot for $\pi^+\pi^+n$ final state: $M^2(\pi_1^+,n)$ versus $M^2(\pi_2^+,n)$.

B. The Reaction $\pi^+p \rightarrow \pi^+\pi^+n$

The analysis of this reaction is similar to that of the reaction $\pi^+p \rightarrow \pi^+p\pi^0$, but the results are strikingly different, primarily because the two mesons in the $\pi^+\pi^+n$ final state must be in a state of isotopic spin 2, which has no known resonances. The Dalitz plot, shown in Fig. 14, exhibits increased density for (π^+,n) effective masses near 1.68 BeV. This is more easily seen in the π^+n mass histogram in Fig. 15. The π^+n spectrum has been fitted with a sum of phase space plus Breit-Wigner-weighted phase space plus the reflection of the resonance onto the other π^+n pair. The best fit is a good one and yields the following parameters:

π^+n effective mass: (see Fig. 15)

percentage of N^*	$(17.2 \pm 2.5)\%$
reflection of N^*	$(17.2 \pm 2.5)\%$
phase space	$(65.5 \pm 4.4)\%$
mass of N^*	1668 ± 13 MeV
width of N^*	168 ± 35 MeV
percent of events containing N^*	$(34.4 \pm 4.4)\%$

It is interesting that we apparently observe the $N_{15}^*(1688)$, but not the $N_{13}^*(1512)$, especially in view of the suggestion³² that the 1512-MeV state may not be a resonance in the usual sense of a 90-deg real phase shift.

To investigate π - π scattering in the $T=2$ state, we have plotted the square of the $\pi^+\pi^+$ mass versus the square of the four-momentum transfer to the neutron (Fig. 16). There is a general enhancement at low Δ^2 for all $\pi^+\pi^+$ masses. This may be caused by single pion exchange with a weak nonresonant $T=2$ π - π scattering vertex [Figure 12(b)].

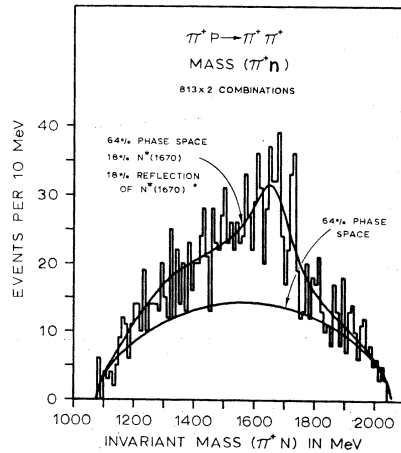


FIG. 15. Invariant mass spectrum of π^+n in $\pi^+\pi^+n$ final state. The N^* peak is at 1668 MeV and has a full width of 168 MeV.

³¹ S. Treiman and C. Yang, Phys. Rev. Letters 8, 140 (1962).

³² J. Helland, C. Wood, T. Devlin, D. Hagge, M. Longo, B. Moyer, and V. Perez-Mendez, Phys. Rev. 134, B1079 (1964).

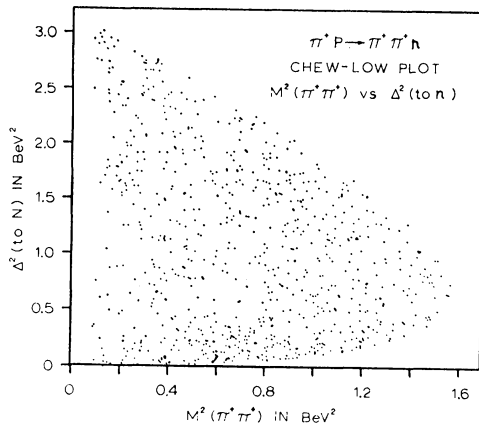


FIG. 16. Chew-Low plot for $\pi^+\pi^+n$ final state: $M^2(\pi^+\pi^+)$ versus four-momentum transfer to neutron.

V. PRODUCTION OF TWO PIONS

A. The Reaction $\pi^+p \rightarrow \pi^+p\pi^+\pi^-$

The final state $\pi^+p\pi^+\pi^-$ is dominated by the $N_{33}^*(1238)$ resonance and by the ρ^0 resonance. The main features of the resonance production are seen in Figs. 17, 18 and 19. Figure 17 clearly shows that the isobar is strongly produced, often with ρ^0 . To fit the π^+p and $\pi^+\pi^-$ mass spectra, several reflection spectra are required; these were computed with a Monte Carlo program. Additional distortions of the mass spectra may arise from the anisotropic decay angular distributions which depend on the unknown polarizations of the resonances, but these were not considered here.

Fits have been made to the π^+p and $\pi^+\pi^-$ mass spectra using those reflections judged most significant. The results are shown in Figs. 10 and 21. The chi-squared value for each fit is about three standard

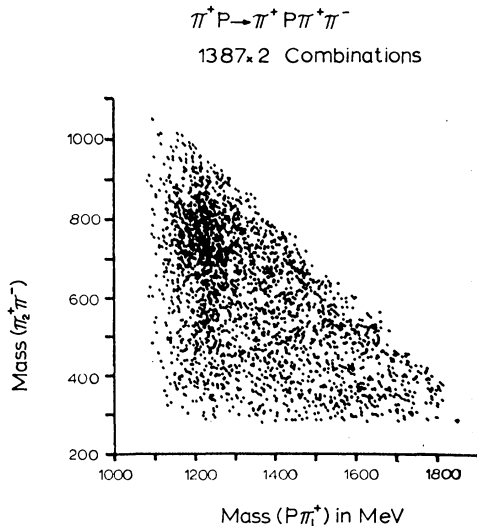


FIG. 17. Invariant mass scattergram for $\pi^+p\pi^+\pi^-$ final state: $M(\pi_1^+p)$ versus $M(\pi_2^+\pi^-)$.

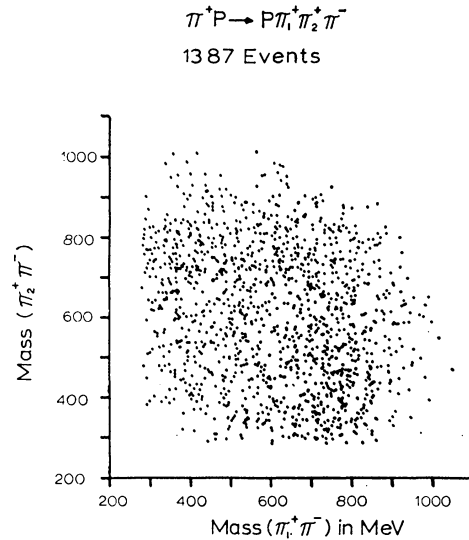


FIG. 18. Invariant mass scattergram for $\pi^+p\pi^+\pi^-$ final state: $M(\pi_1^+p)$ versus $M(\pi_2^+\pi^-)$.

deviations above the expected mean value; the following parameters are derived from the best fits:

percentage of ρ^0 $(35 \pm 7)\%$; mass of ρ^0 765 ± 8 MeV; width of ρ^0 103 ± 13 MeV; percentage of N^* $(68 \pm 10)\%$; mass of N^* 1220 ± 5 MeV; width of N^* 75 ± 8 MeV.

We obtain the cross sections:

$$\begin{aligned} \pi^+p &\rightarrow \pi^+p\pi^+\pi^- & 3.40 \pm 0.11 \text{ mb,} \\ &\rightarrow N_{33}^*\pi^+\pi^- & 2.30 \pm 0.20 \text{ mb,} \\ &\rightarrow \pi^+p\rho^0 & 1.20 \pm 0.20 \text{ mb,} \\ &\rightarrow N_{33}^*\rho^0 & 1.00 \pm 0.20 \text{ mb.} \end{aligned}$$

For the events producing $N_{33}^*\rho^0$, we have plotted the center-of-mass angular distribution of the ρ^0 (see Fig.

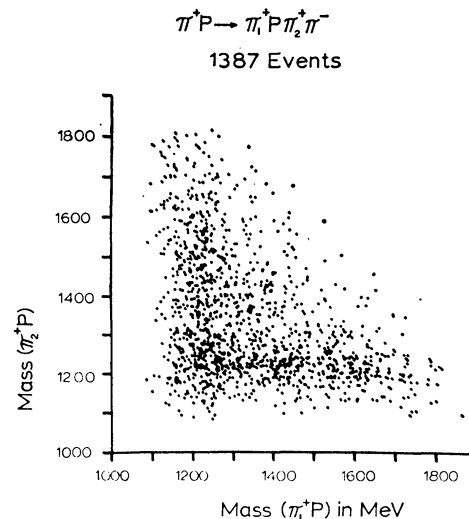


FIG. 19. Invariant mass scattergram for $\pi^+p\pi^+\pi^-$ final state: $M(\pi_1^+p)$ versus $M(\pi_2^+p)$.

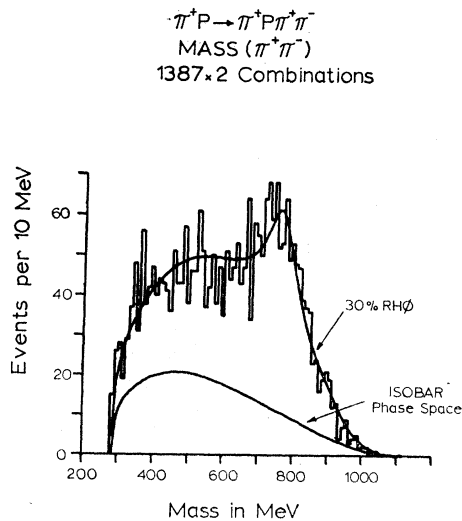


FIG. 20. Invariant mass spectrum of $\pi^+\pi^-$ in $\pi^+p\pi^+\pi^-$ final state. The fitted ρ peak is at 770 MeV with full width 104 MeV.

22). The strong forward peak suggests an exchange process similar to the mechanism proposed for ρ^+ production [Fig. 12(c)]. The Chew-Low plot for the $\pi^+p\pi^+\pi^-$ final state (Figure 23) shows that the $\pi^+\pi^-$ system is produced predominantly at forward angles (i.e., low four-momentum transfer to the $p\pi^+$) when its invariant mass is near the ρ value. This is the expected behavior when the scattering amplitude is dominated by a pole near the physical region.²⁴ Also the Treiman-Yang distribution shown in Fig. 24(d), is isotropic for the $N^*\rho^0$ events, as it must be if they proceed via one-pion exchange.

Figure 24 shows the $\pi\pi$ scattering angle for both ρ^+ and ρ^0 events for low Δ^2 . The momentum transfer spectra for these events are shown in Fig. 25. The Δ^2 cutoffs used were 0.4 BeV^2 for the $N^*\rho^0$ and 0.1 BeV^2 for the $p\rho^+$. As is usually seen,³³ the $\pi\pi$ scattering angle

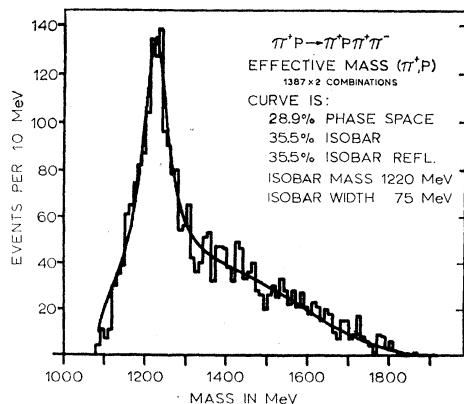


FIG. 21. Invariant mass spectrum of π^+p in $\pi^+p\pi^+\pi^-$ final state.

³³ W. Selove, V. Hagopian, H. Brody, A. Baker, and E. Leboy, Phys. Rev. Letters 9, 272 (1962).

for ρ^0 is very asymmetrical, whereas the distribution for ρ^+ is nearly symmetrical; however, if one deletes the ρ^+ events in which the π^+ and proton form an $N^*(1238)$ isobar [cross-hatched area in Fig. 24(a)], the ρ^+ closely resembles the asymmetric ρ^0 distribution. On the other hand, ρ^+ events in which the π^0 and proton form the $N^{*+}(1238)$ isobar would overpopulate the forward ($\cos\theta > 1$) angles; however, this isobar state seldom occurs in the $\pi^+p\pi^0$ events.

To see if the apparent ρ^0 asymmetry could be caused by interference from ($N^*\pi$) isobar, we have plotted in Fig. 26 the $N^{*++}\pi^+$ and $N^{*++}\pi^-$ mass spectra. The spectra are quite different, as one would expect if the only effect was that of an asymmetric ρ^0 decay, and

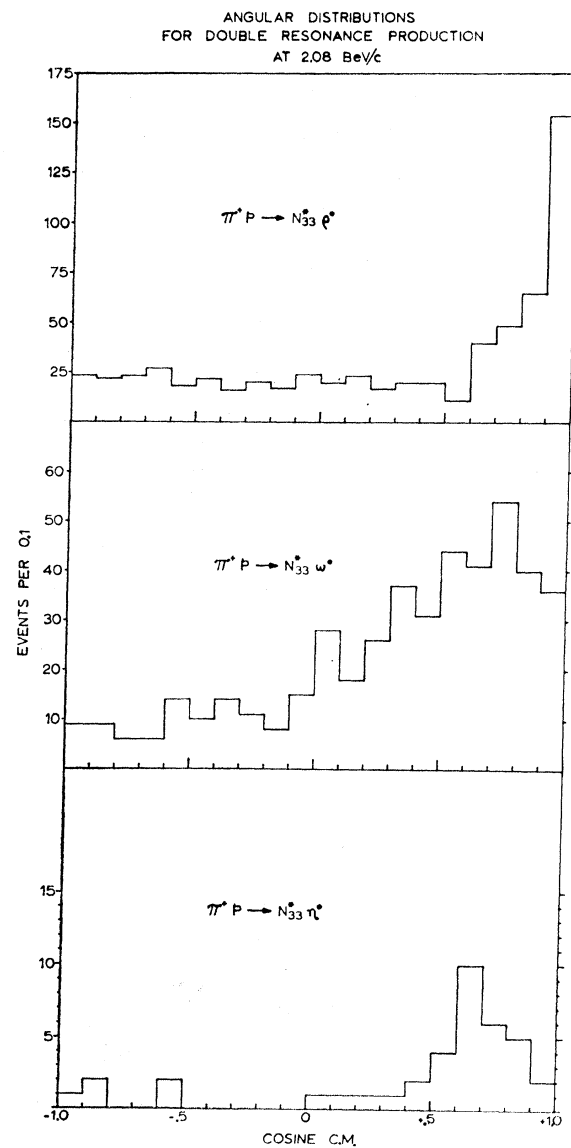


FIG. 22. Angular distributions of $N_{33}^*\rho^0$, $N_{33}^*\omega^0$, and $N_{33}^*\eta^0$ in the production center-of-mass system. Positive $\cos\theta$ represents forward motion of the meson resonances.

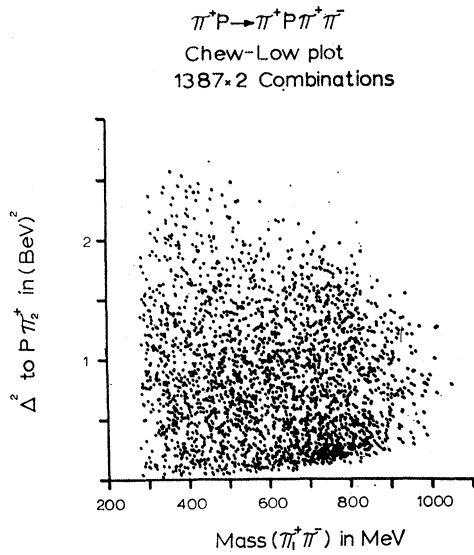


FIG. 23. Chew-Low plot for final state $\pi^+p\pi^+\pi^-$; $M(\pi_1^+\pi_2^-)$ versus Δ^2 (to $\pi_2^+\pi$). Unlike the Chew-Low plot for a three-body final state, the phase-space density of states is not constant over the allowed region of this plot.

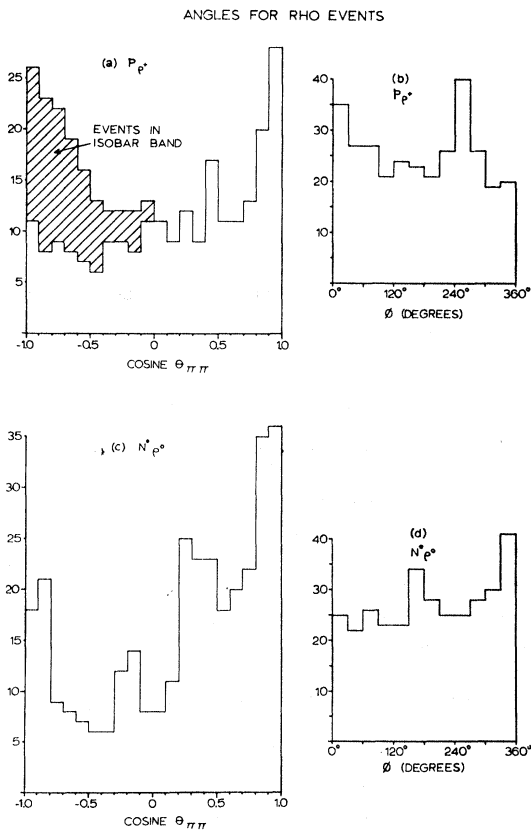


FIG. 24. Polar and azimuthal π - π scattering angles in the two-pion center-of-mass system: (a) Polar $\pi^+\pi^0$ angle for $\pi^+p \rightarrow p\rho^+$ and diagram of Fig. 12(a). (b) Azimuthal $\pi^+\pi^0$ angle for $\pi^+p \rightarrow p\rho^+$ and diagram of Fig. 12(a). (c) Polar $\pi^+\pi^+$ angle for $\pi^+p \rightarrow N_{33}^*\rho^0$ and diagram of Fig. 12(c). (d) Azimuthal $\pi^+\pi^+$ angle for $\pi^+p \rightarrow N_{33}^*\rho^0$ and diagram of Fig. 12(c).

show no significant peaks. The asymmetry in the ρ^0 decay is being investigated further.

Several authors^{13,14,34} have reported resonances in the $\pi\rho$ system; one of these (A_1) has a mass of 1090 MeV which is accessible to our experiment. There is no peak at 1090 MeV in our $\pi^+\pi^+\pi^-$ spectrum. We have made a more careful search by selecting events in which one $\pi^+\pi^-$ pair lies in the ρ^0 peak and the remaining π^+p pair does *not* lie in the isobar peak, plotting the resulting $\pi^+\rho^0$ mass versus four-momentum transfer to the proton. This procedure, used in the above mentioned experiments, favors the diagram in Fig. 12(f) and discriminates against the diagram in Fig. 12(c). The resulting plot (Fig. 27) shows no significant grouping. This is, however, not strong evidence against a resonance, since the diagram of Fig. 12(c) dominates the production

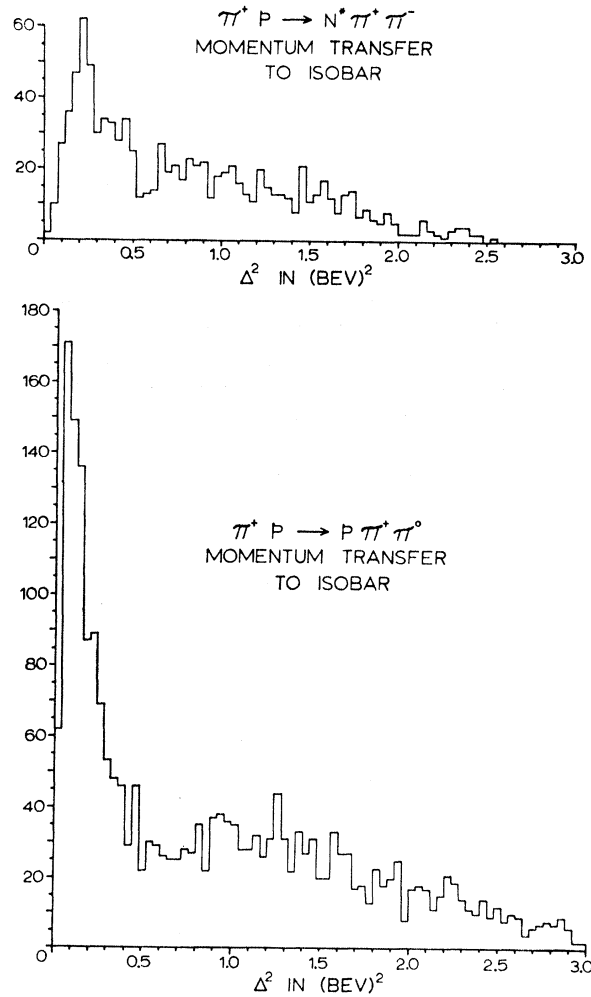


FIG. 25. Momentum transfer to isobar in the reaction $\pi^+p \rightarrow N_{33}^*\pi^+\pi^-$; momentum transfer to the proton in the reaction $\pi^+p \rightarrow p\pi^+\pi^0$.

³⁴ S. Chung, O. Dahl, L. Hardy, R. Hess, G. Kalbfleisch, J. Kirz, D. Miller, and G. Smith, Phys. Rev. Letters 12, 621 (1964).

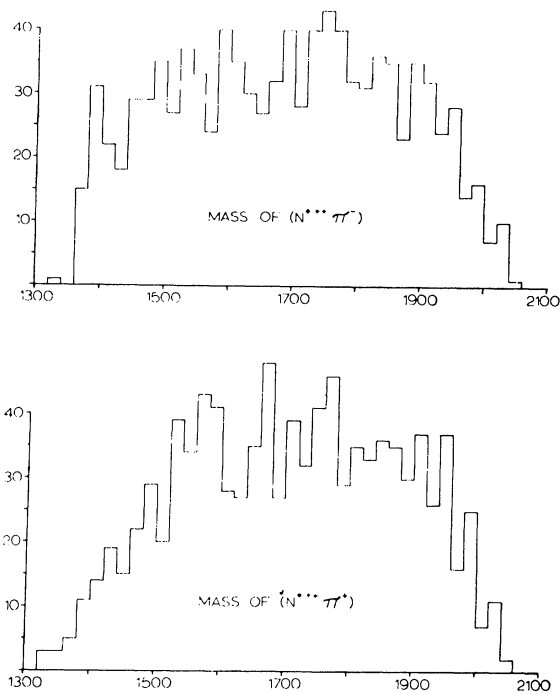


FIG. 26. Effective mass spectra of $N_{33}^{*++}\pi^-$ and $N_{33}^{*++}\pi^+$, for $\pi^+p \rightarrow N_{33}^{*++}\pi^+\pi^-$.

and may produce considerable “background” for the plot of Fig. 27, even after the selection.

Several groups^{35,36} have reported the rare decay mode $\omega \rightarrow \pi^+\pi^-$. Since the ω has odd G parity, the 2π decay mode is forbidden under strong interactions and should occur less often than the decay $\omega^0 \rightarrow \pi^+\pi^-\pi^0$. Moreover, the 2π decay is difficult to observe since the corresponding peak in the $\pi^+\pi^-$ mass spectrum would

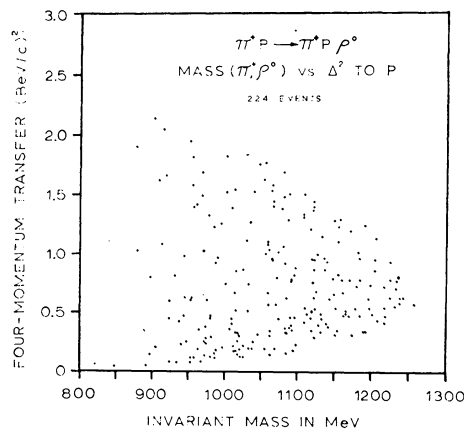


FIG. 27. Search for the A meson: Chew-Low plot for $\pi^+p\rho^0$ final state: $M(\pi^+\rho^0)$ versus Δ^2 (to p).

³⁵ W. Fickinger, D. Robinson, and E. Salant, Phys. Rev. Letters, **10**, 457 (1963).
³⁶ W. Walker, J. Boyd, A. Erwin, P. Satterblom, M. Thompson, and E. West, Phys. Letters **8**, 208 (1964).

fall within the ρ^0 peak near 785 MeV. As shown in Fig. 20, the ρ^0 peak displays no significant irregularities. It has been pointed out³⁵ that one can lessen the ρ^0 “background” by choosing events with high momentum transfer to the remaining particles. When this is done, the $\pi^+\pi^-$ mass spectrum is shown in Fig. 28. The small peak at the ω mass is not statistically significant. Further, this selection has been criticized³⁷ on the grounds that it drastically reduces the statistical significance of the results. Lutjens and Steinberger³⁷ have combined the $\pi^+\pi^-$ mass spectra from several experiments, including this one, and find no peaking in the region of the ω mass, setting an upper limit of 0.8% for the $\omega \rightarrow \pi^+\pi^-$ branching ratio.

On the other hand, Flatte *et al.*³⁸ have recently found evidence for an $\omega \rightarrow 2\pi$ branching ratio of several percent.

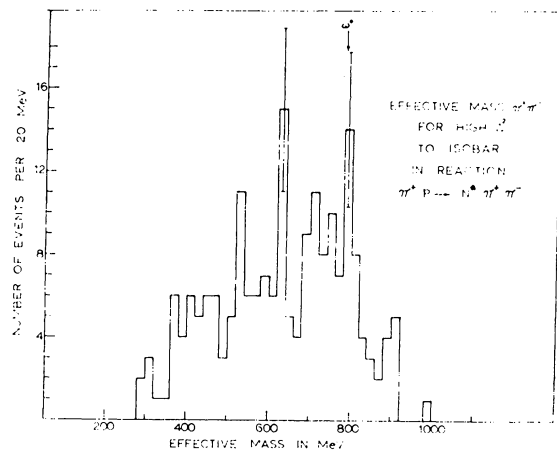


FIG. 28. Search for the $\pi^+\pi^-$ decay of the ω . The invariant mass spectrum of $\pi^+\pi^-$ for final state $\pi^+p\pi^+\pi^-$, selecting only isobar events with high momentum transfer to the isobar.

B. $\pi^+p \rightarrow \pi^+n\pi^+\pi^0$

Although this reaction could proceed by an exchange process similar to that for the $\pi^+p\pi^+\pi^0$ final state, it cannot be studied easily because there are two neutral particles in the final state. We can, however, observe the effective mass of the (n,π^0) and of the (π^+,π^+) ; these distributions are shown in Fig. 29. The slight deviations from phase space may be events with more than one π^0 , which could not be separated from this sample.

VI. THREE-PION PRODUCTION

A. $\pi^+p \rightarrow \pi^+p\pi^+\pi^-\pi^0$

Although this final state is subject to the same problems with reflections as the state $\pi^+p\pi^+\pi^-$, in this case the multipion resonances (ω^0 and η^0) are narrow

³⁷ G. Lutjens and J. Steinberger, Phys. Rev. Letters **12**, 517 (1964).

³⁸ S. Flatte, D. Huwe, J. Murray, J. Button-Schafer, F. Solmitz, M. Stevenson, and C. Wohl, Phys. Rev. Letters **14**, 1095 (1965).

and easier to separate from background (Fig. 30).

Figure 31 shows the effective-mass spectrum for the $\pi^+\pi^-\pi^0$ system (two combinations per event). Because of strong reflections, a sum of phase space and resonance does not fit the mass distribution. However, introducing reflections does not improve the fit greatly, unless one also takes account of the associated production of N^* and ω . When both ω (or η) and N^* are formed, they emerge in opposite directions in the center-of-mass with large momentum difference between the π^+ of the isobar and the $\pi^-\pi^0$ of the ω (or η). This produces a

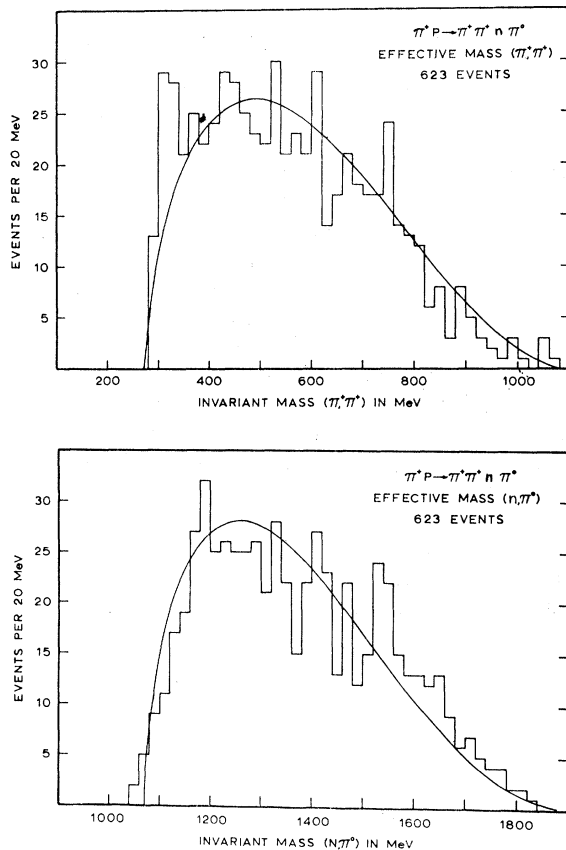


FIG. 29. The $\pi^+\pi^+$ and $n\pi^0$ mass spectra for $\pi^+\pi^+n\pi^0$ final state. Events in which more than one π^0 are produced represent a small contamination.

reflection at high $\pi^+\pi^-\pi^0$ effective mass. Since the η and ω are narrow, the exact shape assumed for the background should not greatly affect the following parameters, which were obtained from the fit to Fig. 31 without reflections.

percentage η^0 ($6.2 \pm 0.6\%$); mass η^0 555 ± 2 MeV; observed width η^0 11 ± 3 MeV; percentage ω^0 ($69 \pm 3\%$); mass ω^0 786 ± 1 MeV; observed width ω^0 25 ± 1 MeV.

From these percentages we obtain the cross section

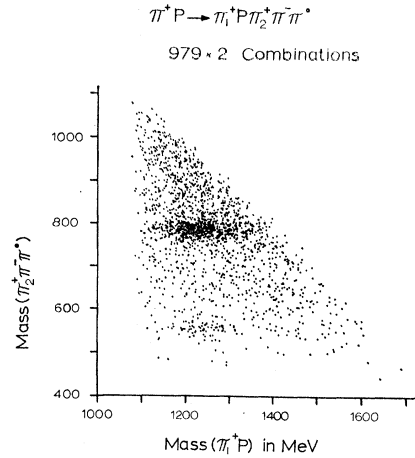


FIG. 30. Invariant mass scattergram for final state $\pi^+p\pi^+\pi^-\pi^0$: $M(\pi^+p)$ versus $M(\pi^+\pi^-)$.

(for the charged decay modes only):

$$\begin{aligned} \pi^+p &\rightarrow \pi^+p\omega_{ch}^0 & 1.66 \pm 0.13 \text{ mb} \\ \pi^+p &\rightarrow \pi^+p\eta_{ch}^0 & 0.15 \pm 0.03 \text{ mb}. \end{aligned}$$

We find that the observed widths of both the η^0 and ω^0 are consistent with the widths of the respective resolution functions, and can set upper limits for the intrinsic widths (to 90% confidence):

$$\begin{aligned} \text{intrinsic width } \omega^0 &< 20 \text{ MeV} \\ \text{intrinsic width } \eta^0 &< 12 \text{ MeV}. \end{aligned}$$

The ω^0 width has been measured by Gelfand *et al.*³⁹ to be 9.5 ± 2.1 MeV. The smallest reported upper limit for the η^0 width,^{2,40} is 10 MeV.

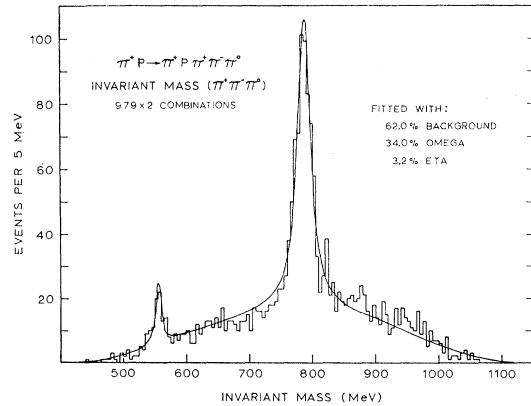


FIG. 31. Invariant mass spectrum of $\pi^+\pi^-\pi^0$ in final state $\pi^+p\pi^+\pi^-\pi^0$: for the fitted curve shown the 62% background is 34% ω reflection, 3.2% η reflection, and only 25% actual non-resonant background. Therefore the actual percentage of omega production is 68%, and for η production 6.4%.

³⁹ N. Gelfand, D. Miller, M. Nussbaum, J. Ratan, J. Schultz, J. Steinberger, T. H. Tan, L. Kirsch, and R. Plano, Phys. Rev. Letters **11**, 436 (1963).

⁴⁰ P. Bastien, J. Berge, O. Dald, M. Ferro-Luzzi, D. H. Miller, J. Murray, A. Rosenfeld, and M. Watson, Phys. Rev. Letters **8**, 114 (1962).

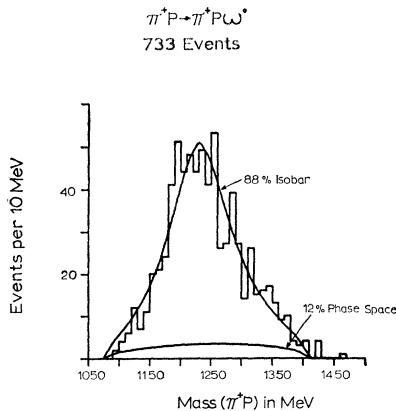


FIG. 32. Invariant mass spectrum for π^+p in final state $\pi^+p\omega$, where the ω decays by the charged mode $\pi^+\pi^-\pi^0$. For events in which both $\pi^+\pi^-\pi^0$ combinations lie in the ω peak, the mass combination nearest to 786 MeV was chosen to be the ω .

The ω , η , and N_{33}^* are the only resonances observed in this reaction; no significant amount of ρ occurs in the $\pi^+\pi^-$, $\pi^+\pi^0$, and $\pi^-\pi^0$ mass plots.

For events which produce an ω , the effective mass spectrum of the remaining π^+ and proton is shown in Fig. 32, which is best fitted with $88 \pm 6\%$ N_{33}^* and $12 \pm 6\%$ phase space. For $N_{33}^*\omega$ single-pion exchange is not allowed (since the $\pi\pi\omega$ vertex cannot conserve G parity) and ρ exchange is the simplest allowed exchange model [Fig. 12(d)].

Comparing Fig. 12(d) with the mechanism proposed for $N^*\rho^0$ production [Fig. 12(c)], we note that both the $\pi\rho\omega$ and $\pi\pi\rho$ vertices are p wave so that they have the same angular-momentum barrier, but since the exchanged ρ is heavier than the exchanged π the $N^*\omega$ production should be less peripheral than N^* production. Indeed, Fig. 22 shows that the ω is peaked less strongly forward than the ρ^0 .

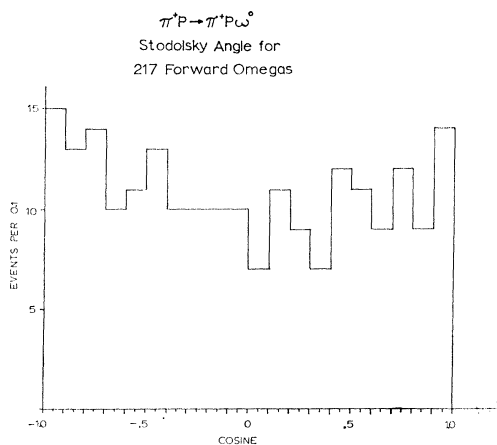


FIG. 33. Stodolsky angle, i.e., the angle between the normal to the decay plane of the ω and the beam pion in the ω rest frame. Only forward ω events have been used, in order to reduce background.

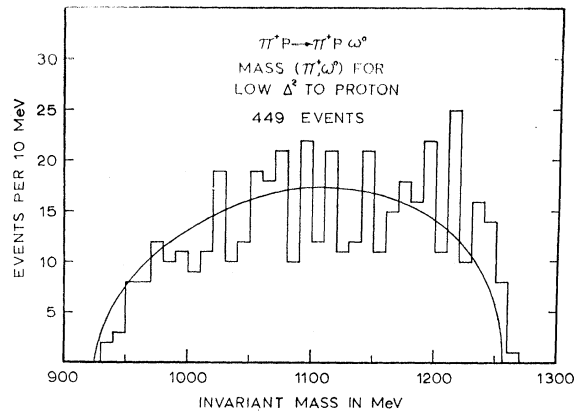


FIG. 34. Search for the B meson: invariant mass spectrum of $\pi^+\omega$ in the final state $\pi^+p\omega$, for events with low momentum transfer to the proton.

Stodolsky⁴¹ has proposed a test for ρ exchange in $N^*\omega$ production, based on the fact that angular-momentum conservation at the $\pi\rho\omega$ vertex implies that the angular momentum of the ω in its own rest frame must have a component along the beam direction. He predicts the distribution $dN/d\cos\theta = 1 - \cos^2\theta$, where θ is the angle between the normal to the decay plane of the ω and the beam direction. As Fig. 33 shows, the $N^*\omega$ events do not obey this distribution.

The angular distribution of the decay plane of the ω , with respect to both the beam direction and the normal to the production plane, is consistent with isotropy for all ω^0 production angles. This suggests little or no polarization of the ω .

A broad resonance (the B meson) has been reported^{12,14} at about 1250 MeV in the $\pi^+\omega$ system. This mass is barely accessible in our experiment. We observe no enhancement in the $\pi^+\pi^+\pi^-\pi^0$ mass spectrum for

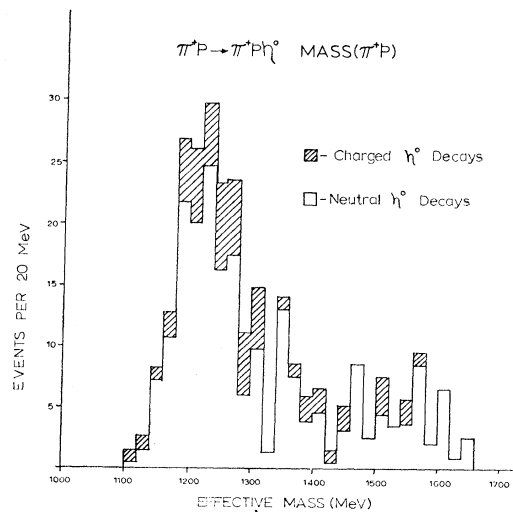


FIG. 35. Invariant mass spectrum of π^+p in final state $\pi^+p\eta$.

⁴¹ L. Stodolsky, Phys. Rev. 134, B1099 (1964).

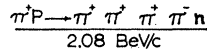
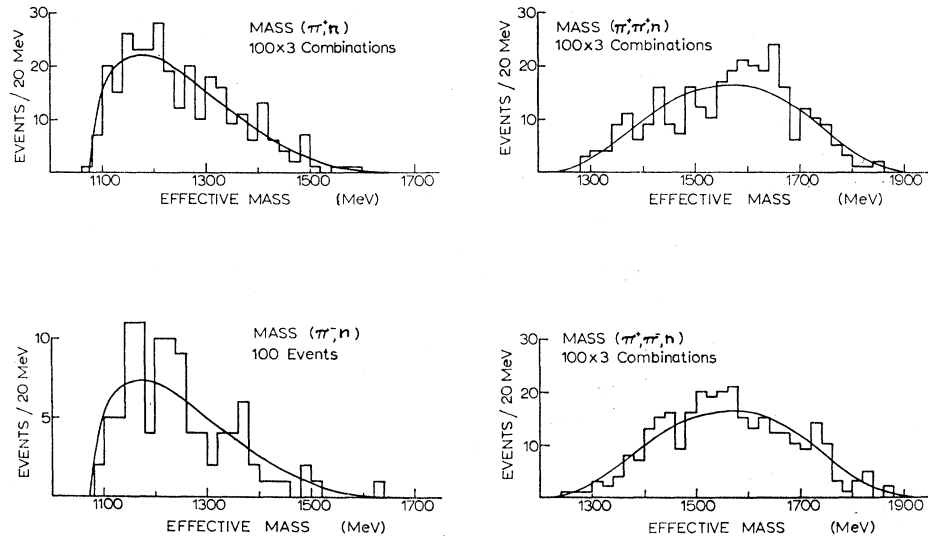


FIG. 36. Invariant mass spectra for final-state $\pi^+ \pi^+ \pi^+ \pi^- n$ combinations involving the neutron.



ω events. Since the original observation of the B showed it to be made chiefly in low-momentum-transfer events, we have selected ω events with low four-momentum transfer to the proton, and plotted the resulting $\pi\omega$ mass spectrum in Fig. 34. The slight enhancement in the high-mass region is probably caused by the N_{33}^* . We conclude that no appreciable amount of B meson is present.

We have selected $\pi^+ p \pi^+ \pi^- \pi^0$ events with neither $\pi^+ \pi^- \pi^0$ triplet in the ω^0 peak, but with at least one $\pi^+ \pi^- \pi^0$ triplet in the η region, and have plotted the effective mass of the other π^+ and the proton in Fig. 35. This spectrum shows that the eta is produced primarily with the $N^*(1238)$ isobar, in contrast with results at higher energies.¹⁰ This is confirmed by the events in which the η decays by its all-neutral modes. For

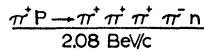
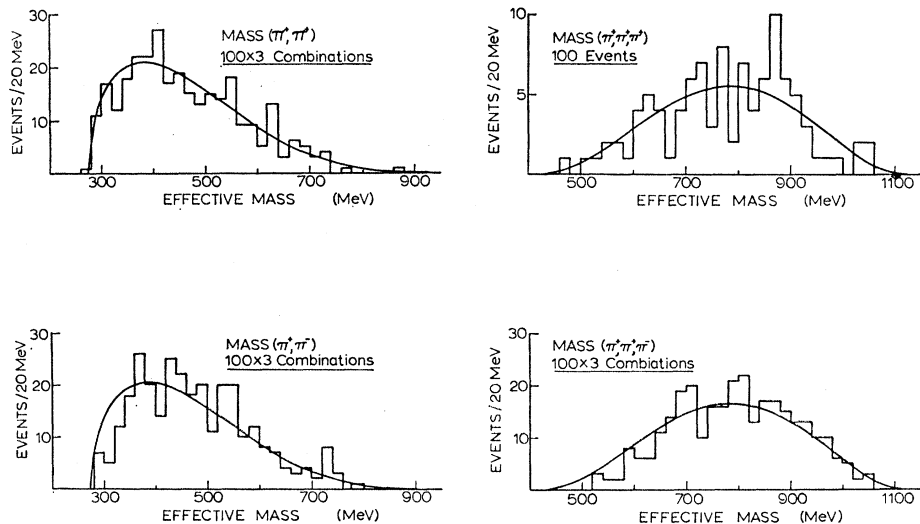


FIG. 37. Invariant mass spectra for final-state $\pi^+ \pi^+ \pi^+ \pi^- n$ combinations involving only pions.



$\pi^+p\pi^+\pi^-\pi^0$ events which form both N^* and η , the center-of-mass angular distribution is shown in Fig. 22. The distribution has a forward peak at $\cos\theta$ equal to 0.7. The corresponding plot for $N^*\eta$ events in which the η decays by an all-neutral mode peaks even more forward; however, the latter distribution is less reliable because of poorer resolution and more background.

We note that η production cannot proceed through single-particle exchange of π , ρ , ω , η , ϕ , or f^0 , if isotopic spin, angular momentum, parity, and G parity are conserved at both vertices. For isotopic-spin conservation, the exchanged particle must be $T=1$, ruling out the η and ω and f ; for G -parity conservation, the G parity must be odd, ruling out the ρ ; and for angular-momentum and parity conservation the exchanged particle must have even spin with even parity or odd spin with odd parity, ruling out the π . The exchange of two pions is also not allowed, because of G -parity conservation. However, exchange of an A_2 meson with quantum numbers $(1)2^{+-}$ is allowed.

B. The Reaction $\pi^+p \rightarrow \pi^+n\pi^+\pi^-\pi^-$

The cross section for $\pi^+n\pi^+\pi^-\pi^-$ is much lower than for $p\pi^+\pi^+\pi^-\pi^0$. This is consistent with the fact that this reaction does not show pronounced resonances. The effective-mass plots, shown in Figs. 36 and 37, reveal no significant deviations from phase space.

VII. DECAY OF THE ρ INTO FOUR PIONS

We have measured the cross sections for production of ρ^+ and ρ^0 in the final states $p\pi^+\pi^0$ and $\pi^+p\pi^+\pi^-$. We also observe the final states $p\pi^+\pi^+\pi^-\pi^0$ and $p\pi^+\pi^+\pi^-\pi^+\pi^-$ and can set an upper limit for the amount of ρ^+ and ρ^0

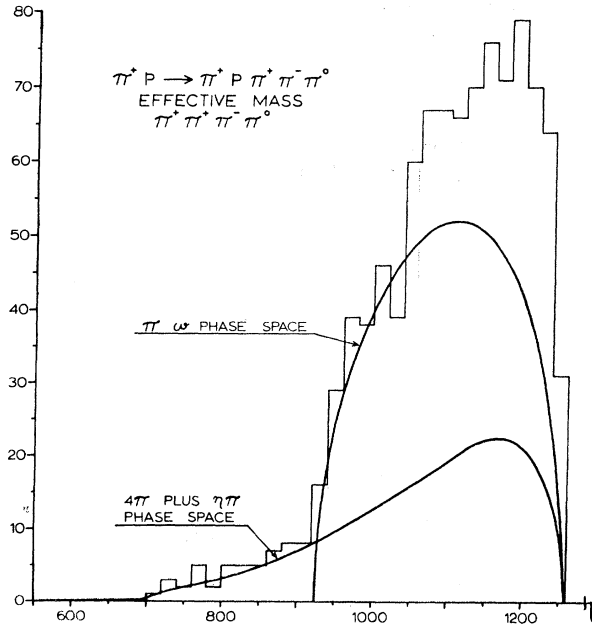


FIG. 38. Effective mass of $\pi^+\pi^+\pi^-\pi^0$ for $\pi^+p\pi^+\pi^-\pi^0$.

in these reactions. Figure 38 shows the effective mass of $\pi^+\pi^+\pi^-\pi^0$ in the final state $p\pi^+\pi^+\pi^-\pi^0$. The phase-space curves are normalized to correspond to the known amounts of η and ω . The spectrum is highly distorted by the presence of the ω^0 , but not in the region of interest for ρ^+ decay. Between 700 and 800 MeV there are 13 events, where one expects 7 from the $\eta\pi$ phase space plus 3 from the 4π phase space. This yields the branching ratio:

$$(\rho^+ \rightarrow \pi^+\pi^+\pi^-\pi^0)/\rho^+ \rightarrow \pi^+\pi^0 = 0.0035 \pm 0.0040.$$

In our film there are only six events with six charged prongs (not counting obvious Dalitz pairs). We have not measured these events, but if *all* of them corresponded to the reaction

$$\pi^+p \rightarrow \pi^+p\rho^0 \rightarrow \pi^+p\pi^+\pi^-\pi^+\pi^-$$

we would have a branching ratio of 0.008 for the ρ^0 to four pions. Therefore:

$$(\rho^0 \rightarrow \pi^+\pi^-\pi^+\pi^-)/(\rho^0 \rightarrow \pi^+\pi^-) \leq 0.008.$$

VIII. PRODUCTION OF NEUTRAL SYSTEMS

About 1200 events were identified as π^+pX^0 , where X^0 is any neutral system with mass greater than two pion masses. The missing mass spectrum from these events is the sum of various many-particle final states. We have therefore computed the effective mass distributions of two, three, and four π^0 mesons produced with a π^+ and a proton, using Lorentz-invariant phase space, and have fitted the observed missing mass spectrum to a sum of variable amounts of these component spectra and of the distributions expected from the all-neutral decay of η and ω . The resulting fit, shown in Fig. 3, is a good one, provided that we make the correction at low masses discussed in Sec. III. From this fit the following parameters are determined:

percentage of $2\pi^0$ (69.5 ± 3.5); percentage of $3\pi^0$ (6.5 ± 2.4); percentage of $4\pi^0 \approx 0$; percentage of η^0 (20.8 ± 2.4); percentage of ω^0 (3.1 ± 1.1); mass of η^0 552 ± 4 MeV; observed width of η^0 53 ± 8 MeV.

The cross sections are:

$$\begin{aligned} \pi^+p \rightarrow \pi^+p\pi^0\pi^0 & 2.31 \pm 0.18 \text{ mb}; \quad \pi^+p \rightarrow \pi^+p\pi^0\pi^0\pi^0 & 0.21 \\ & \pm 0.07 \text{ mb (non-}\eta\text{)}; \quad \pi^+p \rightarrow \pi^+p\eta & 0.69 \pm 0.10 \text{ mb} \\ & \text{(neutral decay)}; \quad \pi^+p \rightarrow \pi^+p\omega & 0.10 \pm 0.03 \text{ mb (neutral} \\ & \text{decay).} \end{aligned}$$

The observed η^0 width is consistent with the resolution. The smaller peak in the ω -mass region is broader and extends to lower masses than the ω peak should. It appears to have two maxima, one at 775 MeV and another at 730 MeV. Unless it is a statistical fluctuation, the 730-MeV peak could be $2\pi^0$ decay of the ϵ^0

meson.^{33,42} This possibility makes the amount of ω^0 difficult to ascertain. The amount quoted was obtained by fixing the ω mass at 785 MeV and varying the amount and width to give the best fit to the missing mass spectrum.

We find the branching ratios: $N_{\text{neut}}/N_{\text{oh}}=4.5\pm 1.0$ and $\omega_{\text{neut}}/\omega_{\text{oh}}=0.06_{-0.02}^{+0.05}$. The ω branching ratio is consistent with other work, but the η branching ratio is higher than the values usually obtained.^{38,43}

The π^+pX^0 events yield a large sample of η mesons to compare with η 's produced in $\pi^+p\pi^+\pi^-\pi^0$ states. We have corrected for background by subtracting distributions from control regions on each side of the η peak. These control regions also provide a rather pure source of $\pi^+p\pi^0\pi^0$ events.

The π^+p mass spectrum for $\pi^+p\eta^0$ states is given in Fig. 35. It verifies that the η is produced predominantly with the N_{33}^* . This is also shown in Fig. 39, where the missing-mass spectrum for isobar events is compared with that for non-isobar events. For the non-isobar events, there is almost no η or ω peak; for isobar

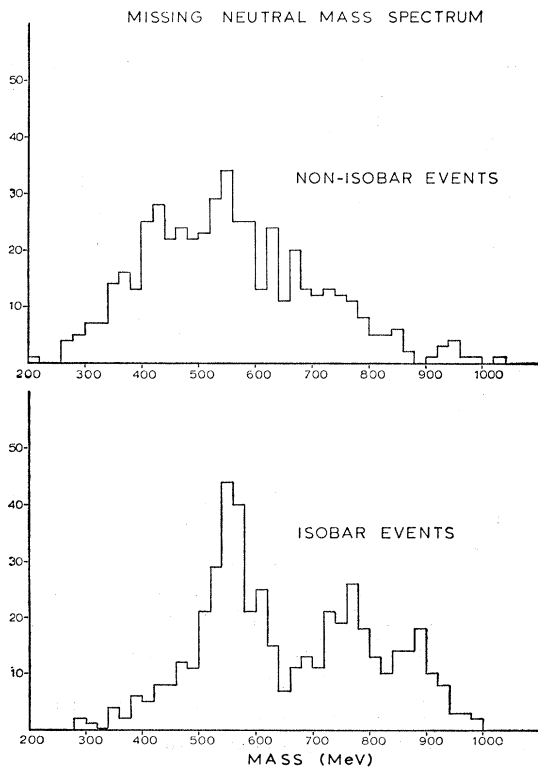


FIG. 39. Missing mass spectra for final state π^+p +neutrals, for the two cases: the π^+p mass lies in the isobar peak (bottom histogram); and the π^+p mass lies outside the isobar peak (top histogram).

⁴² M. Feldman, W. Frati, J. Halpern, A. Kanofsky, M. Nussbaum, S. Richert, P. Yamin, A. Choudry, S. Devons, and J. Grunbaus, Phys. Rev. Letters 14, 869 (1965).

⁴³ A. Rosenfeld, A. Barbaro-Galtieri, W. Barkas, P. Bastien, and J. Kirz, Rev. Mod. Phys. 36, 977 (1964).

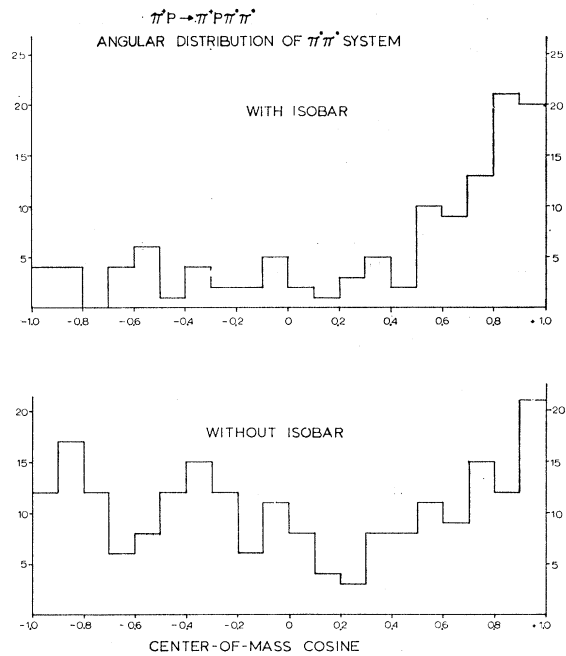


FIG. 40. Angular distributions of the neutral system for the final state π^+p +neutrals, where the missing mass is either between 400 and 500 MeV or between 600 and 700 MeV. These are control regions around the η peak, and also regions where the percentage of $\pi^+p\pi^0\pi^0$ events is very high. Positive cosines represent neutral systems produced forward in the center-of-mass system.

events, the η and ω peaks are prominent and background is greatly reduced.

Using the sample of $\pi^+p\pi^0\pi^0$ events obtained from the π^+pX^0 missing-mass regions outside the η mass, we have plotted the center-of-mass angular distribution of the $\pi^0\pi^0$ system for the $N_{33}^{*++}\pi^0\pi^0$ events and for the non-isobar $\pi^+p\pi^0\pi^0$ events separately. As Fig. 40 shows, the angular distribution of the $\pi^0\pi^0$ system for $N^*\pi^0\pi^0$ events is peaked forward; the non-isobar $\pi^+p\pi^0\pi^0$ events are more nearly isotropic. This suggests the exchange diagram of Fig. 12(e) for the $N^*\pi^0\pi^0$ events.

IX. SUMMARY AND CONCLUSIONS

We have observed resonances through the decay modes:

$$\begin{aligned} \rho^{+,0}(750) &\rightarrow \pi^+\pi^{0,-}, \\ \omega^0(785) &\rightarrow \begin{cases} \pi^+\pi^-\pi^0 \\ \text{all neutrals} \end{cases}, \\ \eta^0(550) &\rightarrow \begin{cases} \pi^+\pi^-\pi^0 \\ \text{all neutrals} \end{cases}, \\ N^*(1238) &\rightarrow \pi^+p, \\ N^*(1668) &\rightarrow \pi^+n. \end{aligned}$$

No other resonances have been detected. We are

slightly above threshold for producing the following resonances which we do not see:

$$\begin{aligned}\phi(1020) &\rightarrow K^+K^-, \\ A_1(1090) &\rightarrow \pi\rho, \\ B(1250) &\rightarrow \pi\omega, \\ X(960) &\rightarrow \eta\pi\pi.\end{aligned}$$

The cross sections for resonance production at 2.08 BeV/c are listed in Table II. The η and ω cross

TABLE II. Cross sections for production of resonant states in π^+p collisions at 2.08 BeV/c.

Reaction	Cross section (mb)
$\pi^+p \rightarrow \rho^+p$	2.07 ± 0.15
$\pi^+p\omega$	1.76 ± 0.16
$N_{33}^*\omega$	1.55 ± 0.20
$\pi^+p\eta$	0.84 ± 0.13
$N_{33}^*\eta$	0.64 ± 0.20
$\pi^+p\rho^0$	1.20 ± 0.30
$N_{33}^*\rho^0$	1.00 ± 0.30
$N_{15}^*\pi^+$	0.77 ± 0.14
$N_{33}^*\pi^0$	0.55 ± 0.08

sections are obtained by adding the cross sections for the charged and neutral decay modes. Figure 41 summarizes published ρ , ω , and η production cross sections in π^+p collisions from 1 to 3.5 BeV/c.

The observed masses and widths of resonances more than about 50 MeV wide may be strongly in-

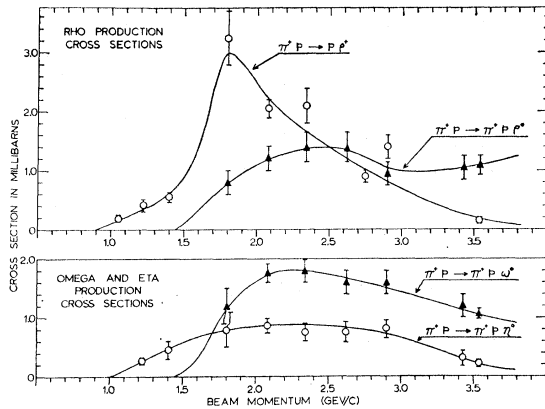


FIG. 41. Cross sections for production of η , ρ , and ω in π^+p collisions from 1 to 3.5 BeV/c. Data are taken from Refs. 1, 2, 10, 12. Values at 1.76 BeV/c are from J. Johnson (private communication).

TABLE III. Mass and width of the N_{33}^* , produced in 2.08 BeV/c π^+p reactions.

Reaction	N_{33}^* peak mass (MeV)	N_{33}^* width (MeV)
$\pi^+p \rightarrow N_{33}^*\pi^0$	1219 ± 5	66 ± 11
$N_{33}^*\pi^+\pi^-$	1222 ± 2	75 ± 6
$N_{33}^*\omega$	1228 ± 4	124 ± 10
$N_{33}^*\eta^+$	1225 ± 6	95 ± 15

fluenced by final state interactions and other dynamical effects. We find that the mass and width of the ρ^+ approach the generally accepted values only for very peripheral collisions. The width of the N_{33}^* varies with the reaction in which it is observed, as shown in Table III.

We have observed that the angular distribution of the meson system is peaked forward in four different two-body inelastic reactions. For the reaction $\pi^+p \rightarrow \rho^+p$, both the Treiman-Yang test and the complete Durand-Chiu calculation are consistent with single- π exchange. For $\pi^+p \rightarrow N^*\rho^0$, the angular distribution of the ρ^0 is similar to that of ρ^+ , which suggests that one-pion exchange dominates here also. For $\pi^+p \rightarrow N^*\omega^0$, π exchange is forbidden, but ρ exchange is allowed. However, this reaction does not satisfy the Stodolsky test for ρ exchange, and the angular distribution is not as forward-peaked as for $N^*\rho^0$. This suggests that single ρ exchange does not predominate in $N^*\omega$ production. For the reaction $\pi^+p \rightarrow N^*\eta$, the angular distribution of the η is peaked forward, indicating that this process may also be peripheral.

ACKNOWLEDGMENTS

We are indebted to Dr. James Sanford for supervising the bubble chamber film exposure of this experiment. Members of the Yale high-energy group, especially Professor Jack Sandweiss and Professor Horace D. Taft, and Dr. Horst Foelsche, Dr. Thomas Ferbel, and Dr. Charles Baltay, contributed valuable assistance and useful discussions. C. Y. Chien identified and analyzed the Dalitz pair events, and David Gadd assisted with identification of other events. We are especially grateful to Dr. Ralph Shutt and the entire staff of the bubble chamber group and the alternating gradient synchrotron at Brookhaven National Laboratory, for their hospitality and cooperation.